

Numerical Study of Integrated Pollutant Control Equipment with Activated Carbon Absorbers

Xiaowen Hao^{1*}, Xiangyu Chao², Yi'e Zhao¹

¹Harbin Institute of Technology at Weihai, School of Automotive Engineering, Weihai, 264209, China

²Harbin Institute of Technology, Harbin, School of Energy Science and Engineering, 150001, China

Received: 4 October 2013

Accepted: 4 November 2013

Abstract

Novel pollutant control equipment, which were called integrated pollutant control equipment, consisted of bag filters and activated carbon (AC) absorbers. The AC absorbers were put forward to absorb the additional pollutants between the old and new emission standards to satisfy Chinese emission standards. The absorbers could be fixed (mobile) bed, annular column, or fluidized bed. The numerical method was employed to simulate the inner flow fields in the integrated equipment. The results show that annular column absorbers can make the flow field more uniform than the others, but its absorption duration has to be discussed. The mobile bed and the annular column absorbers are recommended. The fluidized bed absorber can be applied only if strong heat and mass transfer during absorption are needed.

Keywords: activated carbon (AC), absorber, numerical simulation, uniformity, integrated pollutant control

Introduction

Much work has been done to control fly ash and SO₂ from coal-fired plants at the end of the 11th Five-Year Plan of China, which ended in 2010. NO_x emission control began to draw great attention in recent years. Low-NO_x combustion technologies and flue gas denitration technologies were quickly put into the engineering. But the existing pollutant control technologies face great challenges with the promulgation of the Emission Standard of Air Pollutants for Thermal Power Plants of China (GB13223-2011) from 2012.

The old emission standard (GB13223-2003) for SO₂ was 400 mg/Nm³. The new standard (GB13223-2011) is 200 mg/Nm³ for the old plants and 100 mg/Nm³ for the new plants. The circulating fluidized beds (CFBs) for flue gas desulfurization (FGD) are facing great challenges. They are very hard to satisfy the new standard. So these plants have to spend much capital to improve the CFBs for FGD. And some desulfurization system even has to be rebuilt.

The NO_x emission standard is raised from 650 mg/Nm³ to 100 mg/Nm³ in China. The standard can be satisfied if all of the thermal power plants install selective catalytic reduction (SCR) denitrification reactors. SCR is installed between the exit of the economizer and the entrance of the air preheater. The new plants have the reservation areas for SCR reactors. But installing the SCR reactors into the existing plants is very difficult. And the immense capital for the SCR is another difficulty.

The emission standard for mercury was first proposed in the new standard. Hg has three states: elemental mercury (Hg⁰), divalent mercury (Hg²⁺), and particulate mercury (Hg (p)). The pollutant control equipment can reduce Hg²⁺ and Hg (p) concentration to some degree [1, 2]. But they have little effect on Hg⁰. Controlling Hg⁰ is a key factor if the mercury emission standard is satisfied. So the capital for Hg⁰ removal is essential.

From the analysis above, the additional pollutants between the old and new standards should be removed. But the corresponding investment is large. So simple technologies with low cost without modifying the existing CFBs for

*e-mail: haoxiaowen@gmail.com

FGD, denitration equipments, and other flue gas pollutant control technologies are necessary. The integrated pollutant control technologies belong to these technologies and are attracting more attention [3, 4].

Some of the integrated technologies use activated carbon (AC) as an absorber, which can absorb SO_2 , NO_x , and Hg with high removal efficiency [5, 6]. One of the technologies installs the AC in fixed bed, mobile bed, or fluidized bed to desulfurization and denitration [7, 8]. But they are applied in small-sale power plants, and not scale applied in China because of the high AC price and the large area to install them. The fluidized bed is used less in engineering.

The AC filters are used to remove ozone and organic pollutants from the air [9]. These bag filters, which can be used for several months, are made with fiberglass media lined with AC. But the application of it in coal-fired plants is not appropriate because the bags are often applied for several years in plants and the AC must not saturate during this period.

The difficulties of the integrated technologies by the AC are where to install the AC, how to decrease their modified and operational cost, and how to decrease the apparatus area and pressure drop.

Fog and haze were more frequent at the beginning of 2013 than ever in China. $\text{PM}_{2.5}$ from plants devotes much to the fog and haze. The particles emission standard is raised from 50 mg/Nm^3 for the old standard to 30 mg/Nm^3 for the new standard. Effectively controlling $\text{PM}_{2.5}$ is a key factor to satisfy the new standard. But only bag filters and electrostatic bag filters can satisfy them in the long time running by capturing $\text{PM}_{2.5}$ effectively.

Novel pollutant control equipment, called integrated pollutant control equipment (IPCE), was put forward for these problems. It can be used to remove the additional pollutants between the old and new standards. It is built by modifying the bag filters through adding AC absorbers in these filters. Bags first remove almost all of the particles, and then the AC absorbs other pollutants.

The IPCE with four kinds of absorbers were designed first. Flow regulation is a key factor for the IPCE operation. The uniform flow field is very important for uniform AC absorption. So the flow field of gas-solid phase in the equipment was simulated and optimized.

IPCE with Fixed Bed or Mobile Bed Absorber

Equipment Setup

The filter bag number was 9 for the bag filter. The AC absorber replaced the middle bag and was installed in the middle and top cabinet from Fig. 1. The AC absorber was a fixed bed or counter mobile bed absorber. The bags were inner-filtrate bag-type. Ash on the bags was blown by reverse gas blowing or shaken cleaning technologies. The modification was simple enough so that the transformation from bag filters to the IPCE was very easy, and the corresponding modification cost was low. The area of the IPCE was the same as the bag filter.

The absorber structure of the fixed bed or the mobile bed was the same. The difference of the two beds was the AC stilled or flowed. The absorber was surrounded by a filter screen. The pore size of the filter screen was small enough that the AC in the absorber could not leak, but the flue gas could flow in. The AC was added from the AC bin and flowed down by the star wheel type feeder. The AC was easily changed. The AC could be regenerated for several times. So the operation cost would be low. The AC bottom pipe was imperforated. The flue gas could only flow from the filter screen into the absorber.

The flue gas average velocity U in the absorber must be lower than the AC critical (minimum) fluidization velocity for the mobile bed absorber. The critical fluidization velocity was identified as:

$$u_{mf} = \sqrt{\frac{d_p(\rho_p - \rho_g)g}{24.5\rho_g}} \quad (1)$$

...where u_{mf} is the critical fluidization velocity, d_p is the mean diameter of AC, ρ_p is true density of AC, and ρ_g is the flue gas density.

The minimum absorber diameter can be calculated as

$$D_{AC,min} = \sqrt{\frac{4Q_v}{\pi u_{mf}}} \quad (2)$$

...where $D_{AC,min}$ is the minimum diameter of the absorber and Q_v is the flue gas flux.

The calculated $D_{AC,min}$ was 180 mm. In order to get better removal efficiency, more AC was needed. So the diameter of the absorber was optimized.

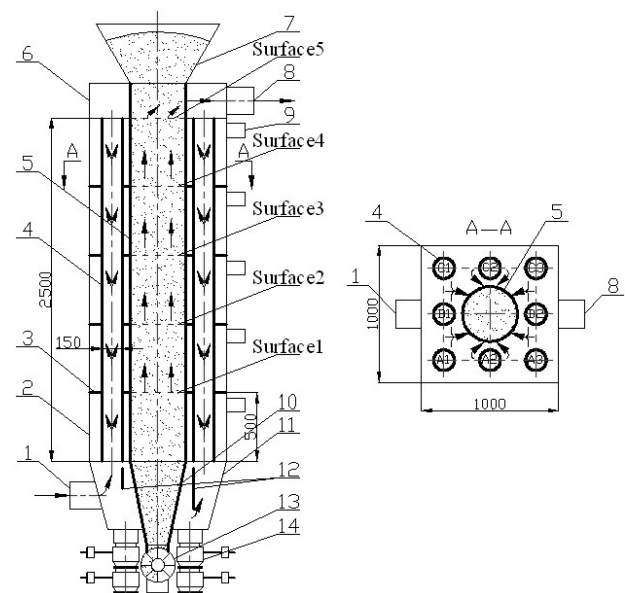


Fig. 1. IPCE with fixed bed or mobile bed absorber.

1. flue gas inlet, 2. middle cabinet, 3. clapboards, 4. filter bags, 5. AC absorber, 6. top cabinet, 7. AC bin, 8. flue gas outlet, 9. reverse gas blowing entrances, 10. AC bottom pipe, 11. ash bunker, 12. guide plates, 13. star wheel type feeder, 14. air lockers.

Simulation Setup

Air was used to substitute the flue gas in simulation. The equipment inlet was set as velocity-inlet and the outlet was pressure outlet. The slip velocity of flue gas and particle was ignored. The standard k-ε model and discrete particle model (DPM) were used to simulate the flow field. The simulation conditions were: uniform inlet velocity distribution, fully developed outlet, unsteady flow field, five-second step time, and standard wall function. The AC bottom pipe was deleted in the simulation because there was no flue gas nor AC absorption.

The flue gas flux Q_v and temperature were set as 500 Nm³/h and 70°C, respectively. The particle diameter fit Rosin-Rammler diameter distributions. The mean fly ash diameter D_f was 91 μm. The boundary condition of bags was set as porous jump, whose parameter was from Wang [10]. The spherical AC was selected. Its bulk density ρ_B was 586.8 kg/m³, its void fraction ε was 0.4645, and its mean diameter d_p was 60 mm, respectively.

The minimum AC velocity is calculated as:

$$U_{c,min} = \frac{UY_1}{\varepsilon Y_1 + X_1^*} \quad (3)$$

...where $U_{c,min}$ is the minimum AC velocity in the absorber, Y_1 is the pollutant concentration at the inlet, and X_1^* is the equilibrium adsorption concentration in the solid phase corresponding to Y_1 [11].

The AC adsorption to SO₂, NOx, and Hg is complex. The equilibrium adsorption concentration of the pollutants is hard to determine. So the value of Y_1 and X_1^* in Eq. 3 refer to the equilibrium adsorption concentration of SO₂ because the SO₂ concentration was much higher than NOx. The operational AC velocity U_c is 1.1-2.0 times higher than $U_{c,min}$ when absorbing SO₂. Higher U_c should be selected when the pollutants are absorbed. So the multiple was selected as 1.5-2.5 times higher than $U_{c,min}$.

The porous media model was used to simulate the AC. Porous media is modeled by the addition of a momentum source term to the standard fluid flow equations.

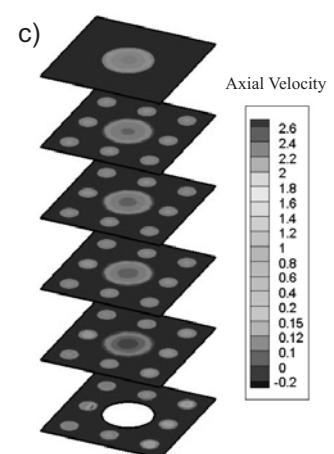
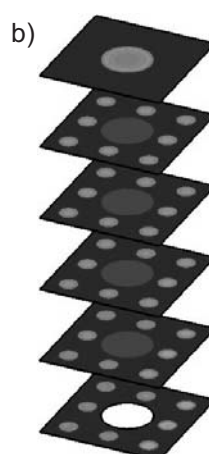
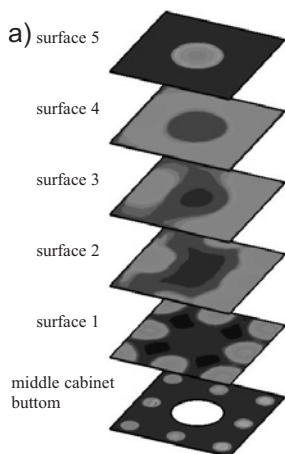


Fig. 2. Axial velocity profile in the middle cabinet cross-section.

(a) with guide plates without clapboards, (b) with clapboards without plates, (c) with clapboards and plates

Table 1. Flux ratio across each absorber surface for the IPCE, %.

Surface number	With guide plates without clapboards	With clapboards without guide plates	With clapboards and guide plates
1	-2.39	5.84	10.27
2	-0.29	6.16	11.94
3	0.18	6.20	12.20
4	0.98	6.41	12.32
5	100	100	100

Results and Discussion

The gas mass flux ratio was defined as the simulated gas mass flux divided by the total flux. It can be seen from Fig. 1 that the absorber was divided into six parts by five plane surfaces in the simulation. The distance of two adjacent surfaces was 500 mm. Surface 5 was the interface of middle and top cabinets. The flux in each surface indicated the flux across this absorber surface.

Optimization of the Equipment Structure

The diameter of the AC absorber as fixed bed was 400 mm in this section. As shown in Fig. 1, based on Hou [12] and many times of simulation, two vertical guide plates with the height of 150 mm and 300 mm were installed in the ash bunker. The middle cabinet of the IPCE had no clapboards originally, which was the same as for the bag filters. But it can be seen from Table 1 that flux ratio in surface 1-4 was very small and even negative. Vortexes could be seen in Fig. 2a. Fly ash filtration and AC absorption were bad with this structure.

Four clapboards at the interval of 500 mm were installed into the middle cabinet out of the bags and the absorber. Fig. 1 shows the four corresponding reverse gas blowing entrances when the bag needed to be cleaned. It can be seen from Table 1 that the flux ratio in surface 1-4 was greatly increased with clapboards without guide plates.

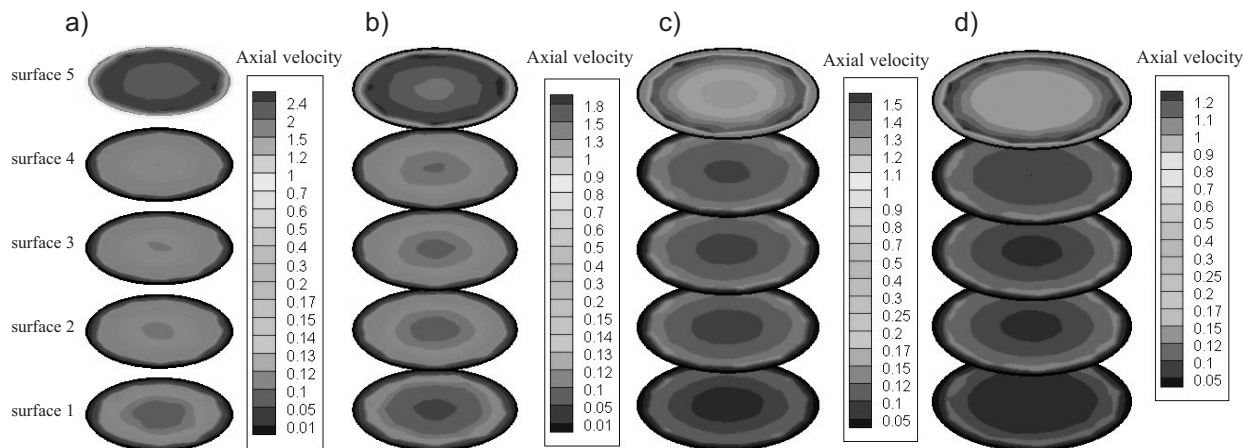


Fig. 3. Axial velocity profile of flue gas in the fixed bed absorber, m/s. (a) diameter of 300 mm, (b) diameter of 350 mm, (c) diameter of 400 mm, (d) diameter of 450 mm

It can be seen from Fig. 2b that the flow with clapboards without guide plates was more uniform than that with guide plates without clapboards. But the flux ratio in surface 5 was much more than the other four surfaces. Most of the flue gas flowed directly to the middle cabinet top, and then flowed into the absorber. The AC in the top of the absorber saturated quickly. But the AC in the lower part of the absorber was far to saturate.

Clapboards and guide plates were both installed. It can be seen from Table 1 that the flux ratio with clapboards and guide plates were higher than the other two structures. It can be seen from Fig. 2c that the flow with clapboards and guide plates was the most uniformity than the other two structures. So uniform AC absorption was much more easily to obtain.

Zhao [13] found that most gas flowed to the filter top before the ash was absorbed in the simulation. The reason was flue gas inertia when each part of one bag’s resistance was set to be same, which was usually supposed in the simulations. The phenomenon may be found for new bags in engineering, too. But for a used bag, the resistance equilibrium of the bag may be determined. That is, more ash is absorbed in the higher part of a bag than lower one. The flue gas with particle can flow through bags uniformly for used bags with a fairly long running time. But the IPCE with clapboards and guide plates can reach uniform particle filtration and AC absorption more quickly for used bags with the optimized flow field.

Pressure drop from the equipment inlet and outlet was compared. The pressure drop of the IPCE with clapboards and guide plates was 13.6% higher than the bag filter. This increasing percentage was acceptable. So the IPCE with clapboards and guide plates was the optimized structure.

Optimization of the Fixed Bed Absorber

The volume of the fixed bed absorber is a key parameter. Greater volume of the fixed bed can hold more AC, which may mean longer absorption time. Greater volume has greater diameter at certain absorber height. But the flue gas may not flow into the middle of the absorber if the

diameter is too large. Thus, optimizing the fixed bed absorber is to get the best absorber diameter by flow simulation.

The absorber diameters in the simulation were from 300 mm to 500 mm. Two standards were used to judge absorption ability. One was the axial velocity profile in the absorber cross-section. The other was the gas flux in the absorber from surface 1 to 4.

It can be seen from Fig. 3 that low axial velocity area was in the middle of the absorber, where the pollutants absorption was bad. The low axial velocity area expanded promptly as the diameter was increased, and the absorption ability from the point of view of axial velocity profile was weakened. So the AC can effectively be utilized with low absorber diameter by Fig. 3.

Fig. 4 shows that gas flux ratio was increased from diameter of 300 mm to that of 500 mm with the same surface number. So the absorption ability from the point of view of flux was strengthened when the diameter was increased.

From the analyses above, we found that the absorption ability of the diameter of 400 mm was best, then the diameter of 350 mm and 300 mm.

Optimization of the Mobile Bed Absorber

The absorber diameter and the AC velocity were used to optimize the absorber. The judging standard was similar to

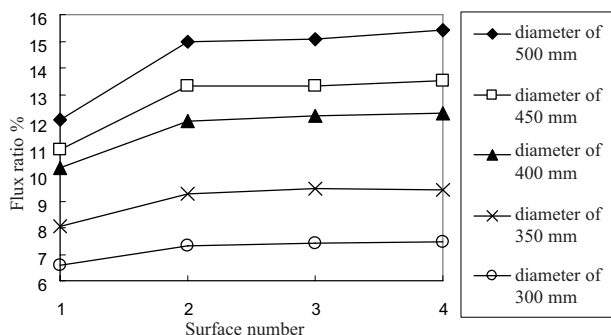


Fig. 4. Gas flux ratio in the absorber surface 1-4.

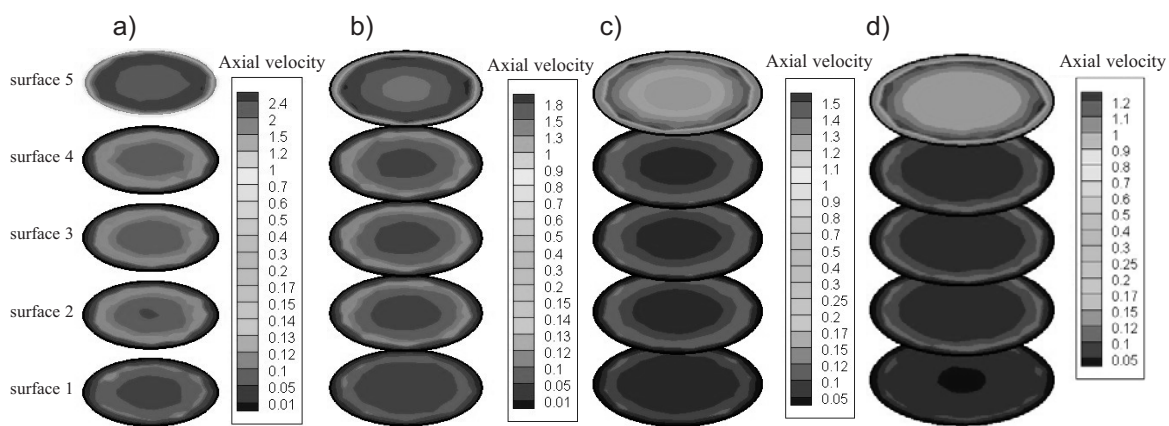


Fig. 5. Axial velocity profile of flue gas in the mobile bed absorber with the AC velocity of 0.028 m/s, m/s. (a) diameter of 300 mm, (b) diameter of 350 mm, (c) diameter of 400 mm, (d) diameter of 450 mm.

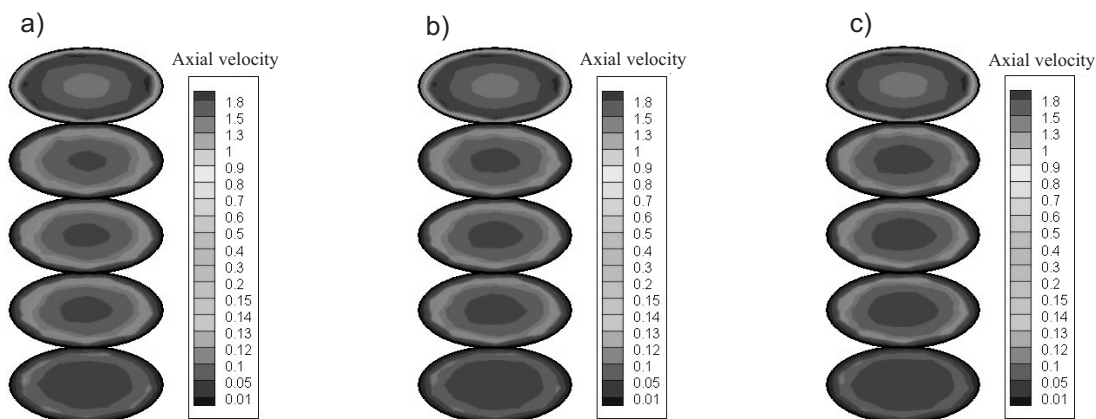


Fig. 6. Axial velocity profile of flue gas in the mobile bed absorber with the absorber diameter of 350 mm, m/s. (a) AC velocity: 0.022 m/s, (b) AC velocity: 0.025 m/s, (c) AC velocity of 0.028 m/s.

the fixed bed absorber. Three kinds of U_c were selected in simulation, which were 0.022 m/s, 0.025 m/s, and 0.028 m/s.

It can be seen from Figs. 5 and 6 that axial velocity area near 0 m/s gradually expanded with larger absorber diameter or higher AC velocity. Small absorber diameter and low AC velocity were good for pollutant absorption. The axial velocity in surface 5 for the diameter of 300 mm was higher than the other diameters. So its flue gas residence time in the absorber was least, which went against pollutant absorption.

The pressure drop was higher for the flowing AC than the static one, but the pressure drop difference was so small that it could be neglected. The flux of the fixed bed and the mobile bed with same absorber diameter was very similar. The absorption ability from the point of view of flux was the same as the fixed bed.

So diameters of 350 mm and 400 mm with the AC velocity of 0.022 m/s were best for AC absorption.

IPCE with Annular Column Absorbers

Equipment Setup

Bag filters with pulse-jet cleaning have been widely applied. IPCE with annular column absorbers were designed

with this ash cleaning technology. The shaken cleaning and reverse gas blowing cleaning style can be utilized in this IPCE, too. The absorbers were installed in the bags for outer-filtrate bag-type, and out of the bags for inner-filtrate bag-type. Fino [14] installed catalytically active ceramic foam candle in each bag. But AC was adapted in this simulation with its excellent absorption ability and its widely applied characteristic. It can be seen from Fig. 7 that the

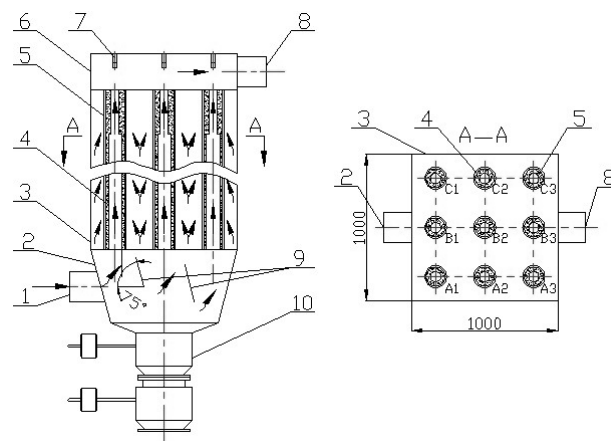


Fig. 7. IPCE with annular column absorbers. 1. flue gas inlet, 2. ash bunker, 3. middle cabinet, 4. filter bags, 5. AC absorbers, 6. top cabinet, 7. injection nozzle, 8. flue gas outlet, 9. guide plates, 10. air locker.

absorbers were installed in each bag. The absorbers were surrounded by two annular filter screens. The AC was installed between the filter screens. There was safe distance between the bags and absorbers to prevent the bags and the absorbers colliding. The interface between the middle and top cabinet was modified to hold the absorbers, and then the absorbers were put directly on the interface. The modification from bag filter to the IPCE with annular column absorbers was simpler than that with the fixed (mobile) bed absorber. The corresponding modification cost was low. The absorbers could be replaced when the pollutants concentration at the IPCE outlet was beyond the national emission standard without replacing the bags.

Two inclined guide plates were installed in the ash bunker. Bag structures were the same as in the ‘Equipment Setup’ section above.

Simulation Setup

The average diameter of AC was set as 2.3 mm. Its void fraction was 0.359. The distance between the bags and the absorbers was ignored in the simulation. The other simulation setup was the same in the as ‘Simulation Setup’ section above.

The effect of pulse-jet cleaning for the IPCE was simulated. It can be seen from Fig. 8 that 2D models were created to investigate the magnitude of the static pressure. The compressed air, which was set as 0.5 MPa, flowed from the mass flow inlet. It generated a short burst of air to clean the equipment. The compressed air flow followed the sine distribution [15]. The 800 ms pulse time was set in one pulse-jet cycle. The flue gas flowed from the pressure inlet and flowed out from the pressure out during the pulse-jet cycle. Bag expansion and contraction were ignored. The distance between the bags and absorbers was not ignored.

Result and Discussion

We have found that most flue gas flowed directly to the bag tops before the ash was collected by the bags. So thickness of the annular column at the absorbers’ top was thickest, and that at the bottom was thinnest. Fig. 9 shows the best absorber structure from many models.

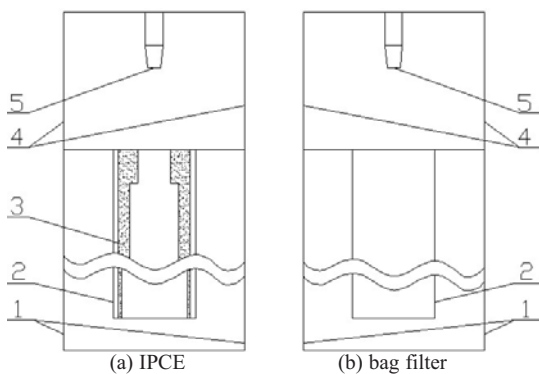


Fig. 8. 2D models of IPCE and bag filter. 1. pressure inlet, 2. bag, 3. AC, 4. pressure outlet, 5. mass flow inlet.

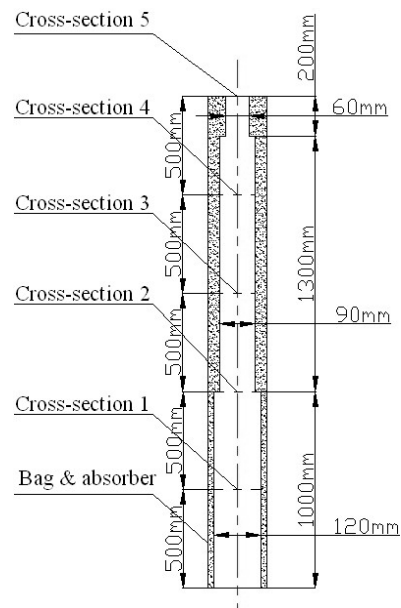


Fig. 9. Structure of the annular column absorber.

Flow Field During Filtration and Absorption

Fig. 10 shows the resultant velocity profile in the center section. Fig. 11 shows the axial velocity profile in the surfaces. Six surfaces in the middle cabinet were selected. The distance of two adjacent surfaces was 500 mm. The lowest surface was the middle cabinet bottom. The highest surface was the middle cabinet top. Much work has been done to optimize the flow field in the bag filter. But the nonuniform flow field was in the bag filter.

The flow field could be quickly uniform for the IPCE. Axial velocity was nearly uniform from surface 3. Those regulations were good for uniform bag filtration and AC absorption.

Fig. 7 shows the bags and absorber number. Fig. 9 shows the position of the five cross-sections of a bag. Fig. 12 shows the flux ratio in cross-sections for the bag filter,

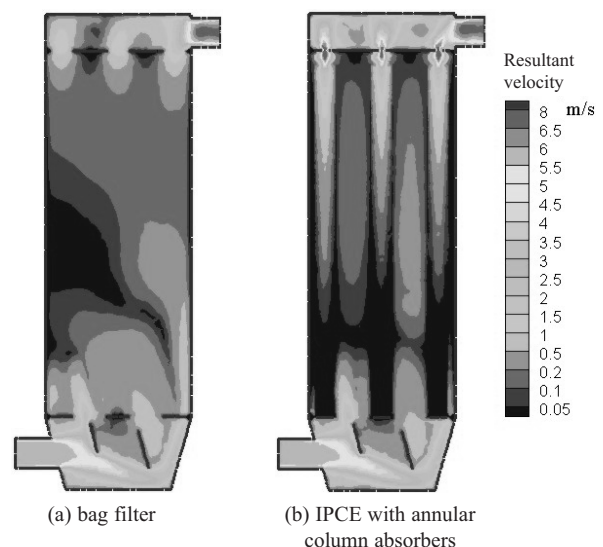


Fig. 10. Resultant velocity profile in the center section.

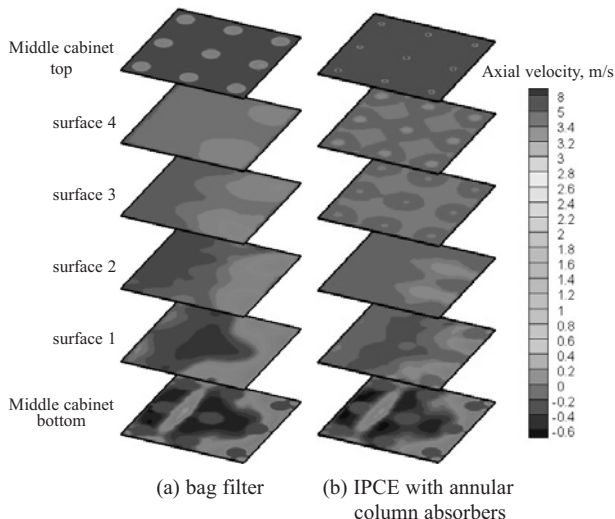


Fig. 11. Axial velocity profile in the surfaces.

which was bad for the uniform bag filtration and bags life-time. Fig. 13 shows the flux ratio in cross-sections for the IPCE. The flux in each cross-section for the IPCE was more regular than the bag filter. The impact from the flue gas to each bag was similar. The AC absorption was similar, too.

The flux nonuniformity coefficient was put forward to analyze the gas flux uniformity of the bags. Smaller nonuniformity coefficients meant more uniformity. The nonuniformity coefficient was defined as the root-mean-square of the flux in the bags (Eq. 4).

$$\zeta = \left[\frac{1}{n} \sum_{i=1}^n \left(\frac{Q_i - \bar{Q}}{\bar{Q}} \right)^2 \right] \quad (4)$$

...where ζ is the flux nonuniformity coefficient, Q_i is the flux of the bags, \bar{Q} is the average flux of the bags, and n is the bag number.

The calculated flux nonuniformity coefficients for the bag filter and the IPCE were 0.013 and 5E-5, respectively. So the uniform bag filtration for the IPCE was easier to get than for the bag filter. The AC absorption was uniform for the IPCE.

The pressure drop for the IPCE with annular column absorbers was 26.6% higher than the bag filter. But the enhance pressure drop was small enough that it can be easily overcome by improving the induced fan.

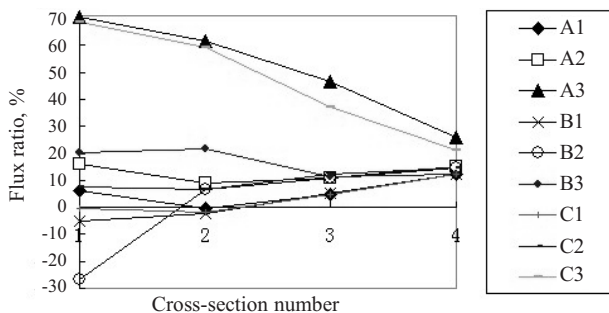


Fig. 12. Flux ratio in cross-section 1-4 for the bag filter.

Static Pressure During Pulse-Jet Cleaning

Fig. 14 shows the calculated relative transient pressures on the bag surface during pulsing. The analysis way referred to Lo [16]. Peak static pressure on the bag surface was used to indicate equipment cleaning ability. The maximum pressure was found when the pulsing time was near 400 msec. The static pressure for the bag filter was larger than that for the IPCE. These findings suggested that unless an alternative process was used to increase cleaning intensity, an increase in cleaning frequency is required to maintain comparative cleaning levels in the IPCE.

Fig. 15 shows the calculated relative transient pressures during pulsing along the IPCE bag. $x/L=0$ represents the bottom location of the bag, and $x/L=1$ the top location. In general, the lowest static pressure was found at $x/L=0.4, 0.9$; and the highest static pressure was at the bottom. This indicates that $x/L=0.4, 0.9$ was a vulnerable spot with a

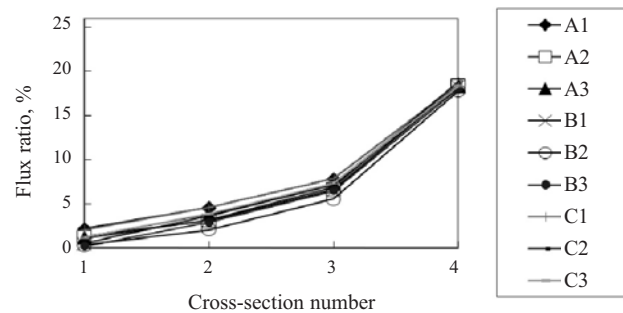


Fig. 13. Flux ratio in bags' cross-section 1-4 for the IPCE with annular column absorbers.

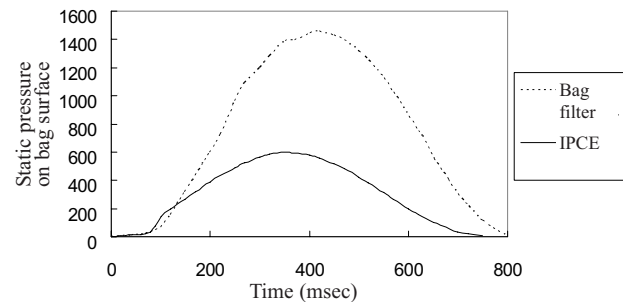


Fig. 14. Calculated relative transient pressures on the bag surface during pulsing.

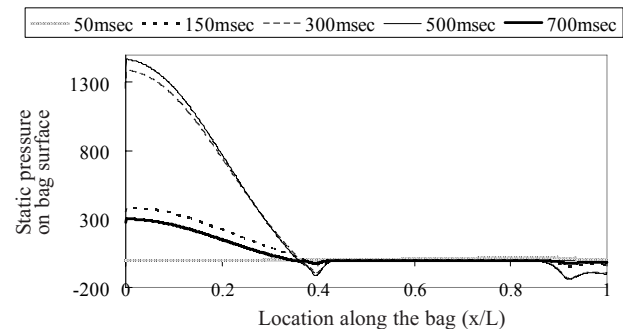


Fig. 15. Calculated relative transient pressures during pulsing at various locations along the bag of the IPCE.

high potential for incomplete cleaning. The negative static pressure was seen in Fig. 15, which was seen in Lo [17]. The use of the clean-on-time mode, which uses a shorter and fixed-time cleaning interval, would probably remedy the problem of incomplete cleaning [18].

IPCE with Fluidized Bed Absorber

Equipment Setup

The fluidized bed absorber has the advantage of high mass transfer compared to the fixed or mobile bed [18, 19]. The IPCE with fluidized bed absorber and shaken filter bags was designed. It can be seen from Fig. 16 that the IPCE was cylindrical. The middle was the fluidized bed absorber. Six bags were uniformly distributed around the absorber. The bags were outer-filtrate bag-types, which were numbered from 1 to 6. The flue gas flowed first from the top cabinet, and flowed through the bags, then flowed into the fluidized bed absorber through bend pipes. The bend pipes were imperforated. The AC was added from the AC recycling pipe to the fluidized bed absorber. The cleaned flue gas after AC absorption flowed into the cyclone, which could separate the AC from the gas. The fresh AC was added from the cyclone bottom. The AC could be recycled to the AC recycling pipe or discharged from the AC outlet. The AC could be regenerated for several times. So the operation cost was low. The fluidized bed absorber could be installed by removing a bag from the bag filter. The cyclone was added into the IPCE. So the modification from the bag filters to the IPCE was not complex. The corresponding modification cost was

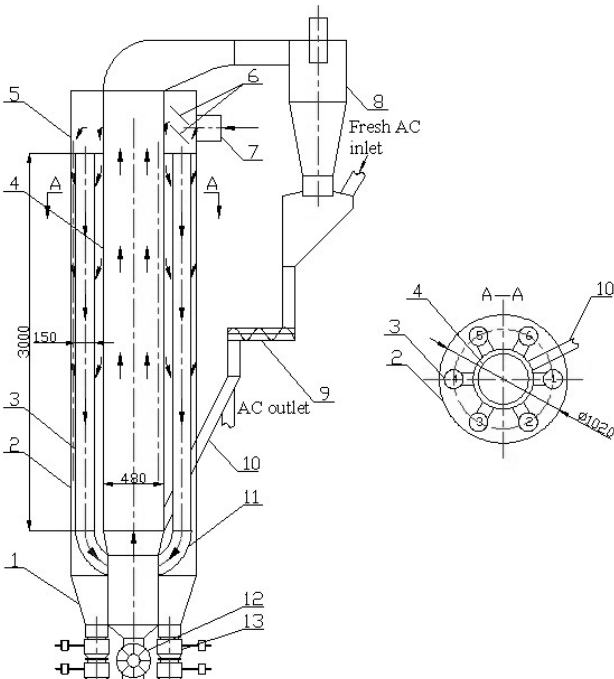


Fig. 16. IPCE with fluidized bed absorber.

1. ash bunker, 2. middle cabinet, 3. filter bags, 4. fluidized bed absorber, 5. top cabinet, 6. guide plates, 7. flue gas inlet, 8. cyclone, 9. screw feeder, 10. AC recycling pipe, 11. bend pipes, 12. star wheel type feeder, 13. air lockers.

Table 2. Flux ratio of each bag and bags' flux nonuniformity coefficient for the IPCE.

Number	1	2	3	4	5	6
Flux ratio, %	17.5	19.2	11.1	19.9	14.6	17.7
Flux nonuniformity coefficient, ζ	0.033					

low. The cyclone area of the IPCE was small. The optimization of this IPCE focused on the uniform bag filtration and AC absorption by the flow field simulation.

Simulation Setup

The average diameter of AC was set at 0.28 mm. The operational fluidization velocity was two times higher than the critical fluidization velocity [19]. The AC was set as solid in simulation. The other simulation setup could refer to the 'Simulation Setup' section above.

Result and Discussion

Guide plates are the usual way to get the flow uniform for the bag filters. We found that a 45° angle for the two guide plates was best from the simulations of many models. The exits of two bend pipes were opposed in order to make the flow in fluidized bed absorber uniform.

Five plane surfaces were used to analyze the flow field in the middle cabinet. The top surface was the middle cabinet top. The distance of the adjacent surfaces was 750 mm.

Fig. 17 shows the velocity profile. The flow field in the IPCE was fairly uniform. Particles from the AC recycling pipe affected the velocity in the fluidized bed absorber, which was the gas flowing to the wall.

Table 2 shows flux ratio of each bag and bags' flux nonuniformity coefficient. The flux across each bag was not very uniform.

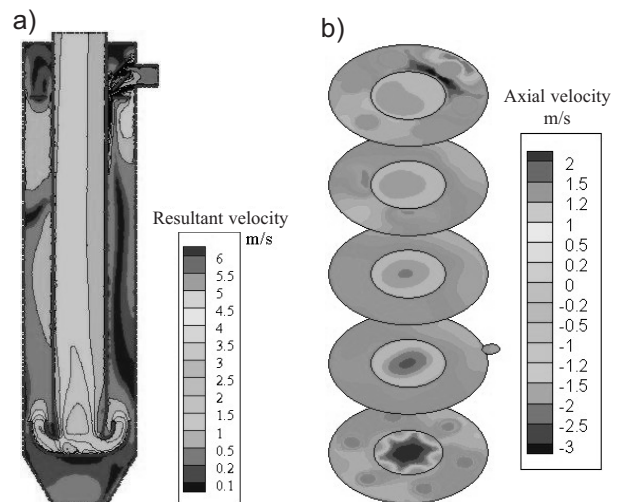


Fig. 17. Velocity profile of IPCE with fluidized bed absorber. (a) resultant velocity profile in the center section, (b) axial velocity profile in the middle cabinet

Comparison of the Absorbers

The structures of the fixed bed and the mobile bed are same. The pressure drop for the mobile bed was a few larger than the fixed bed. The AC absorption efficiency for the mobile bed is higher than that for the fixed bed at the same absorber structure and the operational condition. So the mobile bed is better for the IPCE.

The bags of the IPCE with the fixed (mobile) bed absorber are only inner-filtrate bag-type. The ash cleaning technologies must be reverse gas blowing or shaken cleaning technologies. The fluidized bed absorber can only be applied for the outer-filtrate and shaken bag-type. But the annular column absorber can be installed in all kinds of filter bags.

The modification from the bag filter to the IPCE is easiest for the annular column absorbers, and the most difficult for the fluidized bed absorber. The area for the IPCE with the annular column absorbers is smallest and largest for that with the fluidized bed absorber.

The AC alteration for the annular column absorbers is hardest; the other three kinds of absorbers are easy. The AC in the annular column absorbers is fewest. So its absorption duration may be lower.

The flow field uniformity for the IPCE with the annular column absorbers is best, and then the mobile bed absorber and the fixed bed absorber, that with the fluidized bed absorber is worst.

From the analysis above, the IPCE with the fluidized bed absorber is not recommended. It can be applied only if strong heat and mass transfer during absorbing are needed. The IPCE with the mobile bed and the annular column absorbers are recommended. Their applications depend on the unmodified bag filters.

Conclusions

Structure of the integrated pollutant control equipment with activated carbon absorbers and its operational parameters was preceded and optimized by the numerical study of the flow field. The following results were obtained:

- 1) The integrated pollutant control equipment can be modified from the bag filters easily.
- 2) The operational cost would be low when the AC can be easily recycled for several times. The pressure drop increased by the absorbers was not high.
- 3) Guide plates were useful to optimize the flow field. The annular column absorbers can make the flow field more uniform. The uniform bag filtration and the AC absorption of the IPCE can be largely improved by the flow field optimization.
- 4) An increase in cleaning frequency and the use of the clean-on-time mode are required for the IPCE with the annular column absorbers during pulse-jet cleaning.

Acknowledgements

This work was supported by the Natural Science Foundation of Shandong Province (ZR2013EEM001), the

Fundamental Research Funds for the Central Universities of China (Grant No. HIT. NSRIF. 2013125), and Science and Technology Tackle Key Project of Weihai (2012DXGJ11).

References

1. SRIVASTAVA R.L., HUSTON N., MARTIN B., PRINCIOTTA F., STAUDT J. Control of mercury emission from coal-fired electric utility boilers. *Environ. Sci. Technol.* **40**, 1385, **2000**.
2. KOLKER A., SENIOR C.L., QUICK J. C. Mercury in coal and the impact of coal quality on mercury emissions from combustion systems. *Applied Geo Technologies.* **21**, (12), 1821, **2006**.
3. GAO J.H., CHEN G.Q., LIU J.X., FU X.L., GAO J.M., DU Q., QIN Y. Simultaneous Removal of SO₂ and NO_x by Calcium Hydroxide at Low Temperature: Evolution of the Absorbent Surface Structure. *Energ. Fuel.* **24**, 5454, **2010**.
4. HUTSON N.D., KRZYZYNSKA R., SRIVASTAVA R.K. Simultaneous Removal of SO₂, NO_x, and Hg from Coal Flue Gas Using a NaClO₂-Enhanced Wet Scrubber. *Ind. Eng. Chem. Res.* **47**, 5825, **2008**.
5. HUNG P. C., LO W. C., CHI K. H., CHANG S. H., CHANG M. B. Reduction of dioxin emission by a multi-layer reactor with bead-shaped activated carbon in simulated gas stream and real flue gas of a sinter plant. *Chemosphere.* **82**, (1), 72, **2011**.
6. MA S., YAO J., GAO L., MA X., ZHAO Y. Experimental study on removals of SO₂ and NO_x using adsorption of activated carbon/microwave desorption. *J. Air Waste Manage.* **62**, (9), 1012, **2012**.
7. OLSON D.G., TSUJI K., SHIRAISHI L. The reduction of gas phase air toxics from combustion and incineration sources using the MET-Mitsui-BF activated coke process. *Fuel Process Technol.* **65-66**, 393, **2000**.
8. TSUJI K., SHIRAISHI L. Combined desulfurization, denitrification and reduction of air toxics using activated coke: 1. Activity of activated coke. *Fuel*, **76**, (6), 549, **1997**.
9. BEKO G., FADEYI M.O., CLAUSEN G., WESCHLER C.J. Sensory pollution from bag-type fiberglass ventilation filters: Conventional filter compared with filters containing various amounts of activated carbon. *Build. Environ.* **44**, 2114, **2009**.
10. WANG Y. Analysis and Application of Large-scale Bag Filter Simulation. M.S. thesis, Donghua University. Shanghai, China. **2010**.
11. LI Y. Studies on Reactor of Dry Flue Gas Desulphurization. M.S. thesis, Xi'an University of Architecture and Technology. Xi'an, China. **2006**.
12. HOU W. Study on Gas Distribution Characteristics in Inner-filtrate Bag-type Dust collector. M.S. thesis, North China Electric Power University. Beijing, China. **2006**.
13. ZHAO Y. The Experiment Testing and Numerical Simulation of Flow Field Distribution in a Bag Filter. M.S. thesis, Donghua University. Shanghai, China. **2008**.
14. FINO D., RUSSO N., SARACCO G., SPECCHIA V. A multifunctional filter for the simultaneous removal of fly-ash and NO_x from incinerator flue gases. *Chem. Eng. Sci.* **59**, 5329, **2004**.
15. LOU K. B. The Research on the pulse cleaning of the bag filter with numerical simulation. M.S. thesis, Donghua University. Shanghai, China. **2007**.

16. LO L. HU M.S. C., CHEN D.R., PUI DAVID. Y.H. Numerical study of pleated fabric cartridges during pulse-jet cleaning. *Powder Technol.* **198**, 75, **2010**.
17. LO L.M., CHEN D.R., D. PUI Y.H. Experimental study of pleated fabric cartridges in a pulsejet cleaned dust collector. *Powder Technol.* **197**, (3), 141, **2010**.
18. ZHANG L.Q., JIANG H.T., LI B., CHENG L., MA C. Y. Kinetics of SO₂ adsorption by powder activated carbon using fluidized bed reactor. *Journal of China Coal Society.* **37**, (6), 1046, **2012**.
19. CHIANG B.C., WEY M.Y., YEH C.L. Control of acid gases using a fluidized bed adsorber. *J. Hazard. Mater.* **101**, (3), 259, **2003**.